

〈논문〉 SAE NO. 2000-03-0076

An Investigation about Dynamic Behavior of Three Point Bending Specimen

Jae Ung Cho*, Moon Sik Han**

ABSTRACT

Computer simulations of the mechanical behavior of a three point bend specimen with a quarter notch under impact load are performed. The case with a load application point at the side is considered. An elastic-plastic von Mises material model is chosen. Three phases such as impact, bouncing and bending phases are found to be identified during the period from the moment of impact to the estimated time for crack initiation. It is clearly shown that no plastic deformation near the crack tip is appeared at the impact phase. However, it is confirmed that the plastic zone near the crack tip emerges in the second phase and the plastic hinge has been formed in the third phase. Gap opening displacement, crack tip opening displacement and strain rate are compared with rate dependent material (visco-plastic material). The stability during various dynamic load can be seen by using the simulation of this study.

Key Words : Gap Element, Von Mises Material, Impact Phase, Bouncing Phase, Bending Phase, Gap Opening Displacement, Reaction Force, Plastic Zone, Strain Rate, Visco-plastic Material

Nomenclature

F : Force

D : Gap opening displacement

Subscripts

A and B : middle point A and side point B, respectively

1. INTRODUCTION

In experiments and analyses of dynamic fracture, three point bend specimens are popularly used as in the finite element analyses by Kalthoff¹⁾, Kanninen²⁾, Rosakis³⁾, Van Elst⁴⁾, and Ahmad⁵⁾. Most experiments have been performed by using the drop weight which applies a load to the middle point of a specimen. However, loading rates are somewhat limited in many published

* Member, Department of Automobile, Chonan National Technical College

** Member, Department of Automotive Engineering, Keimyung University

experiments. Therefore, the high speed track with high performance⁶⁾ is used to investigate dynamic fracture behavior of structure under high loading rate. The high speed track used by Wihlborg⁶⁾ can produce impact speeds in the range of 10m/s to 60m/s.

In this paper, computer simulations by using ABAQUS⁷⁾ are utilized to investigate the dynamic behavior of popularly used three point bend specimens under various impact speeds in this paper. The cases with various loading rates applied at the side of the specimen are considered. An elastic-plastic von Mises model with a quarter notch is assumed for mild steel specimen. Gap opening displacement, reaction force, crack tip opening displacement and strain rate are also compared with rate dependent material. The dynamic fracture of material is strongly influenced by the strain rate at the crack tip. The reaction force shows damped oscillations and approaches the quasi-static case. For the impact loading condition in three point bend specimen model, three distinct phases are found by using dynamic finite element method. Three phases such as impact, bouncing and bending phases are found to be identified during the period from the moment of impact to the estimated time for crack initiation. The simulations include plasticity and visco-plasticity behavior of the specimen material. When automobile collides with high speed, stress analysis can be investigated. This result can be applied in most of dynamic fracture of the material.

2. MATERIAL DESCRIPTION AND FINITE ELEMENT MODEL

The material properties of an isotropic elastic-plastic hardening von Mises material is supposed to be the followings. Young's modulus;

$$E = 206 \text{ GPa,}$$

$$\text{Poisson's ratio } \nu = 0.3,$$

$$\text{density } \rho = 7800 \text{ Kg/m}^3$$

$$\text{and yield stress } \sigma_Y = 360 \text{ Mpa.}$$

The stress to strain curve is shown in Fig.1. First yield occurs at 360 MPa as shown in Fig.1.

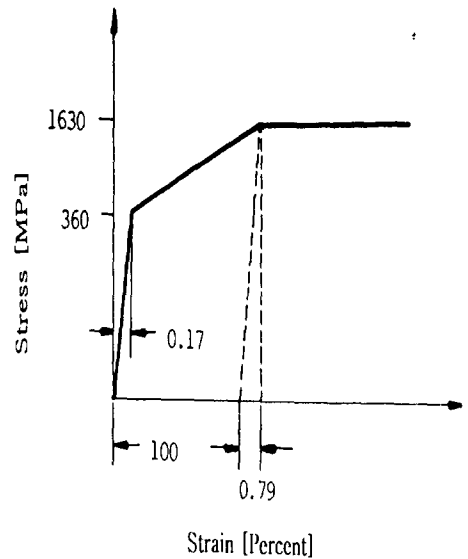


Fig. 1 Static stress-strain curve of the material of a three-point specimen used in our research

The material then hardens to 1630 MPa, after which it is perfectly plastic. Assuming the Young's modulus is 206 GPa, it can be shown that the plastic strain at the 100 percent strain point is 1. The slope during the linear plastic hardening phase is $E' = 1262.2 \text{ MPa}$ until the equivalent von Mises stress reaches 1630 MPa.

The dimensions of the specimen are shown in Fig 2, with the crack length equal to one quarter of the specimen's height. Due to symmetry, only half of the

specimen is considered and a two-dimensional mesh including 92 eight node plane stress element with reduced integration is chosen. The finite element model is shown in Fig.3.

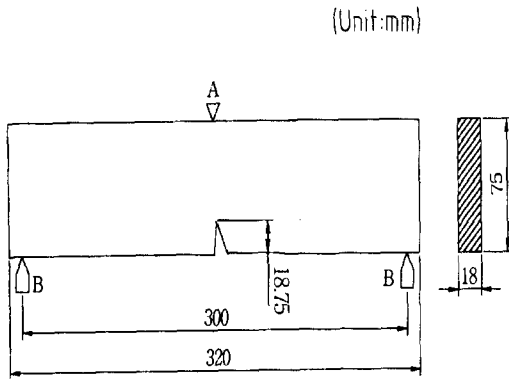


Fig. 2 Three point bend specimen with a quarter notch

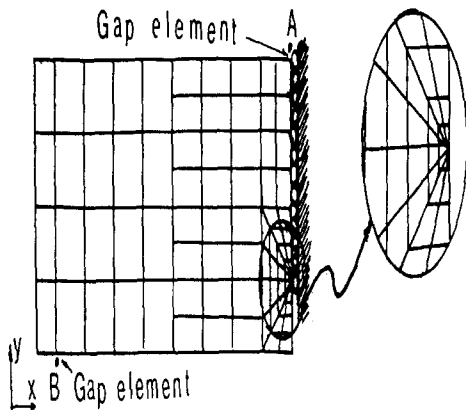


Fig. 3 The finite element model

The model corresponds to load application at the side points B and at the middle point A, respectively. The impact head is assumed to hit the specimen at time zero and its mass is 200Kg. The impact velocity is chosen as $V=15,30,45$ and 60m/s.

This velocity is applied at time zero and is kept constant through the entire calculation. The simulations are performed from the beginning of impact in case of no crack propagation until 600 μs .

The experimental display is also shown in Fig. 4

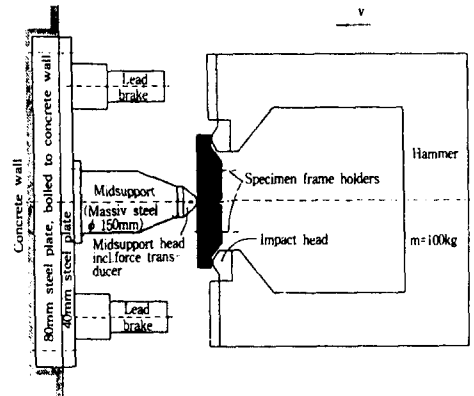


Fig. 4 Cited experimental display

The U-shaped hammer is accelerated to a prescribed velocity and hits the 3PB specimen at its ends. Two hardened and tempered impact heads with cylindrical contact surfaces are attached to the hammer. The experiments of cited paper⁸⁾ were carried with impact velocities of 30 m/s. The mid-support forces for the simulations together with the experimental result are shown with impact velocities of 30 m/s in Fig.5. The simulation including viscoplastic properties is more close to the experimental result. The simulations are combinations of with and without rate influence and with and without crack growth. They are denoted as rate-no rate and crack growth- no crack growth.

Good agreement between the experiments and the numerical simulations was obtained. Therefore, the inspection of this specimen model in this presented paper is sufficient for numerical simulation.

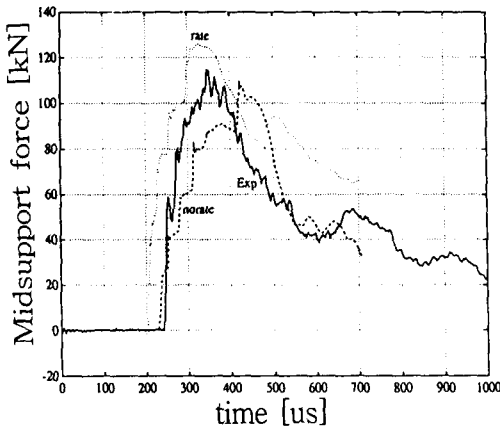


Fig. 5 Mid-support force versus time at 30 m/s impact velocity for the two different simulations and the experiment(experiment :full line, simulations, no rate :broken line, rate:dotted line)

3. SIMULATION RESULTS FOR DYNAMIC BEHAVIOR

The development of the plastic zone is investigated until the estimated time for crack initiation.

3.1 The deformation and reaction force

The reaction forces at the load point B and the support point A and the gap opening displacement at point A are shown in Fig.6 for non-viscoplastic specimen with respect to time. The loading rate for Fig.6 is 15 m/s.

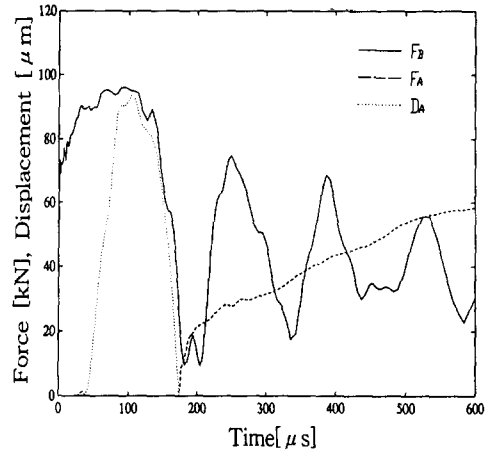


Fig. 6 Dynamic response by impact at the side point B; $V_B=15\text{m/s}$ (no visco-plasticity)
 F_B =Reaction force at B
 F_A =Reaction force at A
 D_A =Gap opening displacement at A

F_B is the force at each one of the point B in Fig.2 and F_A is one half the force at point A.

Immediately after impact F_B increases rapidly to about 70KN and reaches about 97 KN. After about 28 μs the stress wave reaches the support point A, where a small value of F_A is induced during about 10 μs . The specimen then loses contact with the support at point A. The maximum gap opening displacement is about 0.094 mm after 103 μs . At 174 μs after impact, the midpoint gap again closes and F_A increases. F_A grows rapidly to about 20 KN and increases thereafter approximately linearly with time. F_B shows damped oscillations with a period of about 150 μs (this period is reduced slightly with increasing time). At the end of the simulation, the magnitudes of the force at the load and support points are almost the same.

3.2 Three phases and similarities in the dynamics response

It is shown that they behave essentially in the same way. A qualitative division into three different phases, which are named uniquely in this paper, can be made according to Fig.7.

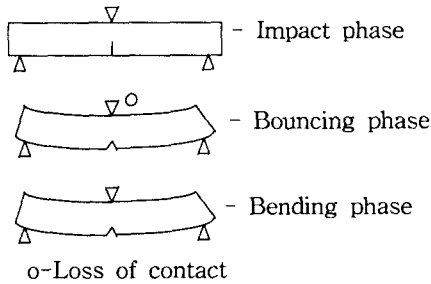


Fig. 7 The three phases

After about $28 \mu s$, the first stress wave reaches the support point, at which a small reaction force is induced. At about $40 \mu s$ after impact, the gap element at the support point opens. This period, from impact up to approximately $40 \mu s$, is named as the "impact phase". No plastic deformation near the crack tip is found before $40 \mu s$. The second phase is called the "bouncing" phase and this phase is sustained until the gap element at the support point closes again. During this phase, the specimen is found to be deformed as a free supported beam by the inertia. This effect was also observed in the experimental investigations⁸⁾.

Examples of the plastic zone shape during the bouncing phase are shown in Fig.8.

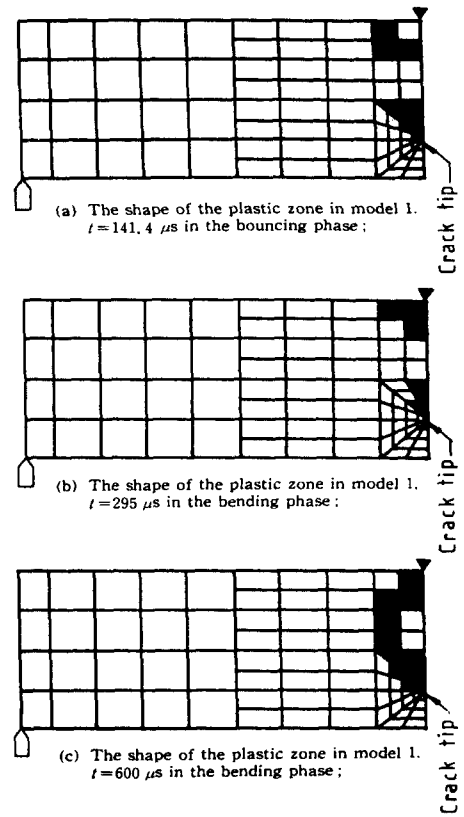


Fig. 8 The shape of the plastic zone in model

The plastic zone size is found to grow during the bouncing phase in Fig.8(a). The third phase is named as "bending phase". This phase starts, as mentioned above, when the gap at the support point closes and reaction force rapidly increases. Fig.8(b) shows the plastic zones at about $300 \mu s$. The areas of the plastic zones in the vicinity of the crack tip and adjacent to point A are found to grow. The reaction force at the side point oscillates around the stable middle point reaction force. The oscillation of the side point force is damped out and approaches the middle

point reaction force(about 50 kN) at the end of simulation. Fig.8(c) shows the plastic zones at 600 μ s. The plastic zones at the middle point A and at the crack tip are linked together by plastic hinge(see Fig.8(c)).

3.3 Reaction Forces and Gap Opening Displacements

Fig.9 shows the change of reaction forces at loading point A and supporting point B and gap opening displacement at A for visco-plastic specimen with time. F_B is the reaction force at point B and F_A is half the reaction force at point A. The loading rate for Fig.9 is 15m/s.

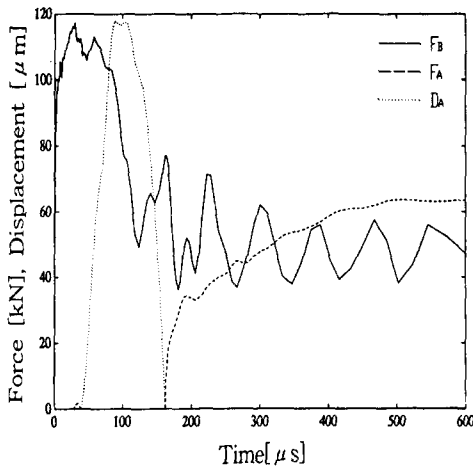


Fig. 9 Dynamic response by impact at the side point B; $V_B=15\text{m/s}$ (visco-plasticity)

As shown in Fig. 6 and 9, reaction forces and gap opening displacements at impacting point B and supporting point A for visco-plastic specimens tend to become higher than those of non-visco plastic specimens.

3.4 Strain rates and CTOD

Figs.10~13 show $\dot{\epsilon}_{xx}$ (strain rate in the x direction) with time of non-visco plastic and visco plastic specimens at positions near the crack tip respectively. Loading rates for Figs.10 and 12 are 30m/s, and those for Fig. 11 and 13 are 60m/s.

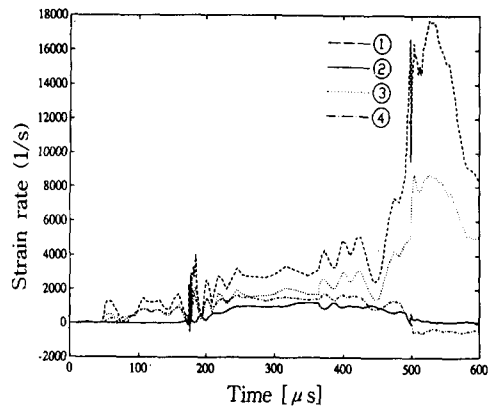


Fig. 10 Strain rate according to time at 1,2,3,4 positions; $V_B=30\text{m/s}$ (no visco-plasticity)

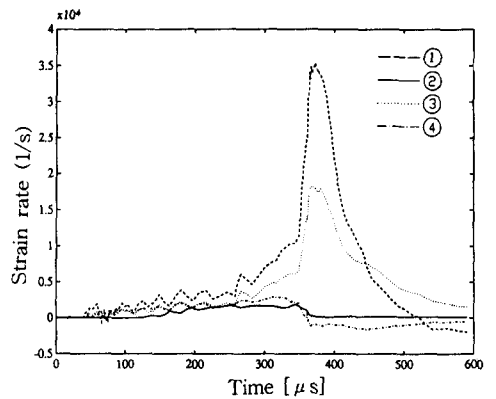


Fig. 11 Strain rate according to time at 1,2,3,4 positions; $V_B=60\text{m/s}$ (no visco-plasticity)

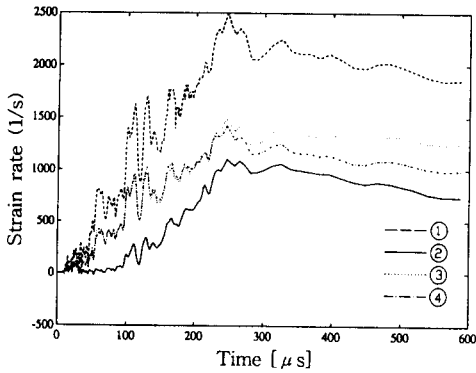


Fig. 12 Strain rate according to time at 1,2,3,4 positions; $V_B=30\text{m/s}$ (visco-plasticity)

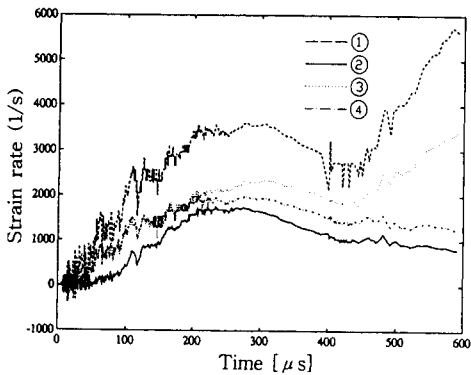


Fig. 13 Strain rate according to time at 1,2,3,4 positions; $V_B=60\text{m/s}$ (visco-plasticity)

The positions at the crack tip are denoted by ①, ②, ③, and ④ as in Fig.14.

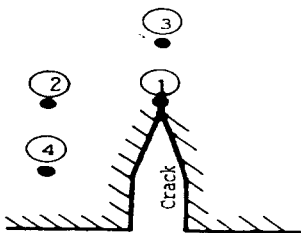


Fig. 14 The positions near crack tip

In Figs. 10~11 and Figs.12~13, dashed lines(---), solid lines(—), dotted lines(⋯), and dot-dashed lines(- · · · -) represent strain rates at the positions ①, ②, ③, and ④, respectively as shown in Fig. 14. We can notice that $\dot{\epsilon}_{xx}$ at the position ① has the largest value and determines the fracture by dynamic crack. For non-visco plastic specimens as shown in Figs.10~11, the strain rate reach maximum values in shorter times as loading rates increase. For visco-plastic specimens as shown in Figs.12 ~13, maximum strain rates increase and occur later with loading rates increasing. In general, maximum strain rates for non-visco plastic specimens are much higher than those for visco-plastic specimens. This information on the tendering of strain rates is useful for predicting fracture time by dynamic crack.

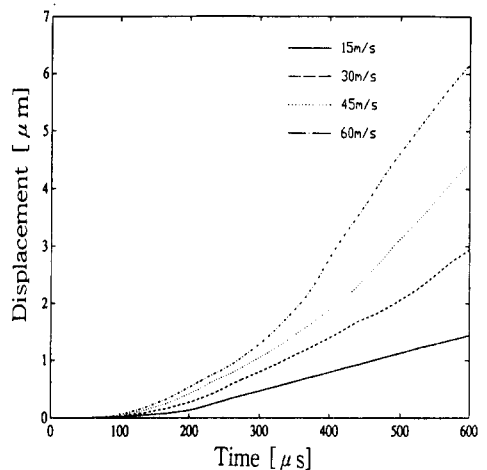


Fig. 15 Crack tip opening displacement according to time at various loading rates; $V_B=15,30,45,60\text{m/s}$ (no visco-plasticity)

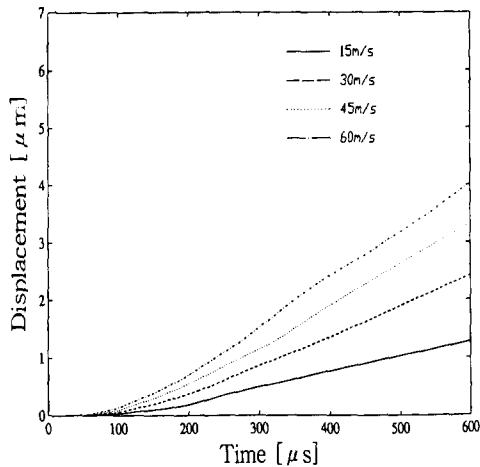


Fig. 16 Crack tip opening displacement according to time at various loading rates;

$$V_B=15,30,45,60\text{m/s(visco-plasticity)}$$

Figs. 15 and 16 are crack tip opening displacement(CTOD) curves with time for non-visco and visco-plastic specimens, respectively with loading rates of 15, 30, 45, and 60m/s.

From Figs.15~16, we can notice that CTOD increases with increasing loading rate irrespective of visco-plasticity of material. However, CTOD of a visco-plastic specimen becomes smaller than that of a non-visco plastic specimen.

4. CONCLUSIONS

The results of computer simulation analysis for the three point bend specimen of mild steel under various dynamic loading conditions are summarized as follows:

1) The specimen is impacted and the first stress wave reaches the support point during the impact

phase. This results in loss of contact between the specimen and the support roller.

2) During the bouncing phase, the specimen is bounced away from the support roller and back again. The plastic hinge in the vicinity of the crack tip starts to form and grows.

3) The oscillation is damped out and approaches the middle point reaction force at the end of simulation.

4) Reaction forces and gap opening displacements at impacting and supporting points of visco-plastic specimens are larger than those of non-visco plastic specimens.

5) As loading rates increase, the maximum strain rates at the crack tips occur earlier for non-visco plastic specimens but occur later for visco-plastic specimens.

6) The maximum strain rate and CTOD of visco-plastic specimens are rather smaller than those of non-visco plastic specimens.

REFERENCES

- 1) J.F. Kalthoff, "On Some Current Problems in Experimental Fracture Dynamics", Workshop on Dynamic Fracture, W. G. Knauss, etc., pp.11-35, 1983.
- 2) M.F. Kanninen, etc., "Dynamic Crack Propagation under Impact Loading", Nonlinear and Dynamical Metrology, San Diego, California, 1988.
- 3) A.J.Rosakis, etc., "Caustics by Reflection and their Application to Elastic-Plastic and Dynamic Fracture Mechanics", SPIE Conference on Photomechanics and Special

- Resistance at Instrumented High Velocity Gas-gun Impact Tests on SENB-Specimens " , ICF 6 , Vol.5, pp. 3089-3097, 1984.
- 4) H.G.van Elst, "Assessment of Dynamic Fracture Propagation Fracture Mechanics, ASME AMD35, pp. 185-200, 1979.
 - 5) J.Ahmad, etc., " Elastic-plastic Finite Element Analysis of Dynamic Fracture", Eng. Frac. Mech.,Vol.17, No. 3 , pp. 235-246, 1983.
 - 6) G. Wihlborg, "Design and Application of a Rig for High Energy Impact Tests ", IUTAm Symposium, Tokyo, Japan, 1985.
 - 7) ABAQUS Manual,Version 4.8, Hibbit, Karlsson and Sorensen, Ino.1989. -
 - 8) Ouk S. Lee, et al., "Dynamic Crack Growth in 3PB Ductile Steel Specimens," Technical Report, LUTFD2, TFHF-3045, Lund, Sweden, 1991.